THE ASTRONOMICAL JOURNAL, 121:2752–2757, 2001 May
© 2001. The American Astronomical Society. All rights reserved. Printed in U.S.A.

ON THE DIFFERENCE BETWEEN TYPE E AND TYPE A OH/IR STARS

J. H. HE AND P. S. CHEN
Yunnan Observatory, Chinese Academy of Sciences, Kunming 650011, China; United Laboratory of Optical Astronomy, CAS; National Astronomical Observatories, China; hjh@cosmos.ynao.ac.cn, iras@public.km.yn.cn
Received 2000 October 12; accepted 2001 January 17

ABSTRACT

The observed spectral energy distributions of a sample of 60 OH/IR stars are fitted using a radiative transfer model of a dusty envelope. Among the whole sample, 21 stars have reliable phase-lag distances, while the others have less accurate distances. L_*-P, $\dot{M}$-P, and $\dot{M}$-L_* relations have been plotted for these stars. It is found that type E (with an emission feature at 10 μm) and type A (with an absorption feature at 10 μm) OH/IR stars have different L_*-P and $\dot{M}$-L_* relations, while both follow a single $\dot{M}$-P relation. The type E stars are shown to be located in an area without large-scale dense interstellar medium, while the type A stars are probably located in dense interstellar medium. It is argued here that this may indicate that the two types of OH/IR stars do not share the same chemical composition or zero-age main-sequence mass and so evolve in different ways. This conclusion has reinforced the argument by Chen et al., who reached a similar conclusion from the Galactic distribution of about 1000 OH/IR stars, based on *IRAS* low-resolution spectrometer spectra.

Key words: stars: AGB and post-AGB — stars: evolution — stars: mass loss

1. INTRODUCTION

Recently, Chen et al. (2001) published a catalog of OH/IR stars with *IRAS* low-resolution spectrometer (LRS) spectra. They also argued that many type E OH/IR stars that are located at high Galactic latitude will never evolve into type A OH/IR stars. In order to examine the differences between the two groups of OH/IR stars (types E and A), this paper is an attempt to investigate the luminosity-period relationship and the relation between mass-loss rate and period for the two groups by radiative transfer modeling. The observed data and the radiative transfer model used are described in §§ 2 and 3, and a detailed discussion of the derived quantities and conclusions can be found in § 4.

2. DATA

A sample of 60 OH/IR stars with known distances was collected from the literature; 36 of them belong to type E, and 18 belong to type A. For the purpose of comparison, three type H stars (red continuum), two type U stars (unusual spectrum), and one type F star (featureless) were also included. The observational spectral energy distribution (SED) of each star consists of three parts: near-infrared (NIR) photometry taken from ground-based observations, *IRAS* far-infrared (FIR) photometry, and *IRAS* LRS spectrum. The LRS spectra are from the on-line *IRAS* Data Analysis Facility of the University of Calgary. The FIR fluxes are obtained from the CD edition of the published *IRAS* Point Source Catalog, and only those fluxes with good quality ($Q \geq 2$) are used. The NIR photometry data of 21 OH/IR stars are given by Xiong, Chen, & Gao (1994), and that for the remaining 39 stars are taken from other papers. References for the NIR photometry data are listed in Table 1. The NIR data are corrected for interstellar extinction. The formula of van Herk (1965) is used:

$$A_V = 0.14 \csc |b| [1 - \exp(-10d \sin |b|)] , \quad (1)$$

where b is the Galactic latitude and d is the distance from the Sun. We also use the method of Cardelli, Clayton, & Mathis (1989) to calibrate the data at different wavelengths.

The periods of pulsation for 46 stars from Chen et al. (2001) were also searched. Twenty-one sample stars have so-called phase-lag distances (this is the most accurate distance available for OH/IR stars up till now; hereafter, these stars are called the phase-lag sample, and the entire collection of 60 stars is called the whole sample), and these distances are taken from Baud & Habing (1983), Herman, Burger, & Penninx (1986), and van Langevelde, van der Heiden, & van Schooneveld (1990). The distances of the other stars are taken from other papers where they are estimated by other methods, e.g., the kinematic method, using the L_{OH}-R^2 relation, and so on, and so they are not very accurate (error can be larger than 100%). The references for distance are listed also in Table 1. For the phase-lag sample the periods, expansion velocities, and phase-lag distances are shown in Table 2.

3. MODELING

3.1. *Model Description*

The radiative transfer model of a spherical dusty envelope is used to fit the observed SEDs. The model used was originally compiled by Szczerba et al. (1997). This code is able to calculate the emerging flux spectrum of a spherical shell observed at a specified distance when the luminosity (L_*) and effective temperature (T_{eff}) of the central star and dust species, dust condensation temperature (T_{cond}), dust density distribution ($\rho_d \sim r^{-n}$), grain size distribution, and the geometric sizes of the envelope are given. The original code was slightly modified so as to make it possible to vary only five quantities when fitting SEDs—T_{eff}, T_{cond}, τ_V, n, and Y_{max}—while the other quantities are fixed at their typical values: astronomical silicate grains, whose electric permittivity and magnetic permeability are taken from Draine & Lee (1984) and Draine (1985); grain size distribution of interstellar dust as $n(a) \sim a^{-3.5}$ with the grain size range from $a_{min} = 0.005$ μm to $a_{max} = 0.25$ μm (Mathis, Rumpl, & Nordsieck 1977). Here τ_V is the total optical thickness at 550 nm, n is the index of negative exponential density distribution law, and Y_{max} is the relative geometric thickness R_{max}/R_{min}. The extinction coefficient and the

TABLE 1

REFERENCES FOR NIR AND DISTANCE DATA

IRAS Name	NIR	Dist.	*IRAS* Name	NIR	Dist.	*IRAS* Name	NIR	Dist.
01037+1219.....	1	2	14297−6010.....	2	10	23412−1533.....	5	10
01304+6211.....	1	2	15193+3132.....	11	12	23425+4338.....	11	6
03293+6010.....	3	4	16474−4418.....	2	10	15255+1944.....	1	8
03336−7636.....	5	6	16494−4327.....	2	10	18182−1504.....	15	7
03507+1115.....	5	7	17073−4225.....	2	10	18257−1000.....	13, 15, 16	17
04140−8158.....	5	6	17073−3955.....	2	10	18257−1052.....	13, 18, 19	17
05098−6422.....	5	6	17271−3425.....	2	10	18276−1431.....	2	7, 8
05528+2010.....	1	8	17317−3331.....	2	10	18348−0526.....	1	17
06500+0829.....	9	6	17360−3012.....	2	10	18431−0403.....	2, 20	17
07209−2540.....	5	10	17540−1919.....	9	12	18432−0149.....	2, 19, 20	7
07585−1242.....	5	6	18135−1456.....	2	7	18445−0238.....	2, 16, 18	7
09425+3444.....	11	6	18437−0643.....	2	7	18460−0254.....	2, 13, 16, 18	7
09429−2148.....	5	4	19017+0608.....	3, 13	4	18488−0107.....	13, 18, 20, 21	17
10189−3432.....	5	6	19059−2219.....	5	10	18498−0017.....	9, 16, 18, 19	17
10287−5733.....	2	10	20000+4954.....	3	7	18549+0208.....	20	17
10580−1803.....	5	6	20077−0625.....	5	10	18560+0638.....	1	17
12310−6233.....	2	10	20259−4035.....	14	12	19039+0809.....	1	7
13157−6421.....	2	10	21206−4054.....	14	12	19192+0922.....	22	17
14086−2839.....	5	12	22516+0838.....	5	10	19550−0201.....	5	8
14247+0454.....	5	7	23041+1016.....	5	12	22177+5936.....	1	7

REFERENCES.—(1) Xiong et al. 1994; (2) Nyman, Hall, & Le Bertre 1993; (3) Sun & Zhang 1998; (4) Bowers, Johnston, & Spencer 1983; (5) Fouqué et al. 1992; (6) Ortiz & Maciel 1996; (7) Herman et al. 1986; (8) Baud & Habing 1983; (9) Lepine, Ortiz, & Epchtein 1995; (10) Le Sidaner & Le Bertre 1996; (11) SIMBAD database; (12) Nguyen-Q-Rieu et al. 1979; (13) Baud et al. 1985; (14) Whitelock et al. 1994; (15) García-Lario et al. 1997; (16) Evans & Beckwith 1984; (17) van Langevelde et al. 1990; (18) Jones, Hyland, & Gatley 1983; (19) Schultz, Kreysa, & Sherwood 1976; (20) Gehrz et al. 1985; (21) Kwok, Hrivnak, & Boreiko 1987; (22) Fix & Mutel 1984.

albedo of the dust grains are calculated from Mie theory. In order to fit the observed SEDs, 2475 models have been calculated by varying $T_{\rm eff}$ from 1300 to 3800 K, $T_{\rm cond}$ from 800 to 1000 K, τ_V from 0.1 to 80, n form 1.4 to 2.6, and $Y_{\rm max}$ from 10^3 to 10^5.

3.2. *Model Fitting*

The models calculated above are used to fit the observed SEDs simply by weighted linear interpolation. The weights are given larger for LRS spectrum and FIR data and smaller for the NIR data because the NIR fluxes are varied for most sample stars. After having derived $T_{\rm eff}$, τ_V, n, $Y_{\rm max}$, and the best-fit model SED for each star from above, it is easy to determine the luminosity (L_*) and gas mass-loss rate ($\dot{M}$) (when the outflow velocity is known) by assuming the dust-to-gas mass ratio to be 10^{-3} for all stars. Here it should be pointed out that the mass-loss rate is calculated at the inner border of the circumstellar shell, and hence this

TABLE 2

SOME PARAMETERS OF THE STARS WITH PHASE-LAG DISTANCES

IRAS Name	Period (days)	V_e (km s^{-1})	D (kpc)	L_* (10^3 $L_\odot$)	$\dot{M}$ ($M_\odot$ yr^{-1})	LRS Spectral Type
01037+1219.....	660.0	18.2	0.74	24.56	0.96	E
05528+2010.....	368.3	2.7	1.20	76.86	0.11	E
15255+1944.....	425.1	7.5	3.10	105.71	0.58	E
19039+0809.....	284.2	6.6	0.29	3.46	0.02	E
18431−0403.....	717.0	17.5	1.45	8.36	0.24	E
19550−0201.....	394.8	5.4	0.85	27.20	0.06	E
01304+6211.....	1995.0	11.0	2.90	50.91	6.86	A
18348−0526.....	1566.0	14.0	1.44	18.09	4.50	A
18560+0638.....	1424.0	16.1	2.04	22.31	4.93	A
22177+5936.....	1215.0	14.5	2.38	14.54	5.58	A
18182−1504.....	1011.7	20.5	0.55	0.84	0.78	A
18257−1052.....	1129.5	18.2	5.06	13.09	2.04	A
18257−1000.....	1975.2	19.0	8.51	83.31	18.99	A
18276−1431.....	890.0	12.0	2.08	3.09	0.60	H
18432−0149.....	1038.6	17.5	7.70	40.99	8.26	A
18445−0238.....	853.0	17.0	1.09	1.46	0.58	A
18460−0254.....	2064.4	19.5	1.77	9.67	3.59	A
18488−0107.....	1540.2	20.6	11.87	81.31	16.32	A
18498−0017.....	1536.3	15.9	5.02	22.58	1.58	H
18549+0208.....	840.0	13.6	4.21	6.30	0.91	A
19192+0922.....	552.0	16.1	1.13	13.82	0.52	A

quantity is theoretically in the simultaneous measure with the luminosity of the center star. Some derived quantities of the phase-lag sample stars are also listed in Table 2.

4. ANALYSIS OF THE FITTED RESULTS

First, the luminosity-period relation (L_*-P relation) for the phase-lag sample of OH/IR stars is shown in Figure 1. As can be seen, for both type E and A stars the luminosity seems to be larger for longer period, but the luminosities for the two types seem to be going along parallel paths, that is, the two L_*-P relations do not join smoothly with each other from that of the type E to that of the type A as we expected. However, it is difficult to draw any convincing conclusion from Figure 1, because too few type E OH/IR stars are included. The same figure for the whole sample is displayed in Figure 2, where many more type E stars are included. This figure is proved to confirm the conclusion of Figure 1. The L_*-P relation does follow different tracks for the type E and A OH/IR stars, although the dispersion in the L_*-P relation is large for both types. In both Figures 1 and 2, type H stars are located in type A region and seem to follow the L_*-P relation of type A stars.

The L_*-P relation of OH/IR stars and Mira variables has been addressed by many authors (Whitelock, Feast, & Catchpole 1991; Le Bertre 1993; Blommaert et al. 1998), but all of them considered only a small number of OH/IR stars and took them as a single class. Here we divide the OH/IR stars into different subclasses according to their *IRAS* LRS spectral classification, and more stars have been included. This gives us the chance to see some inner structure of the L_*-P relation for OH/IR stars, as described above.

The relation between mass-loss rate and period (the $\dot{M}$-P relation) for the whole sample is plotted in Figure 3. It is easy to see that the whole sample follows a single $\dot{M}$-P relation, and, as we already know, the mass-loss rates increase from type E stars with shorter periods to type A stars with longer periods. A similar $\dot{M}$-P relation has been found before for M-type stars by some other authors, e.g., Whitelock et al. (1994). It should be noted that one star is located far from the majority; it is IRAS 18304−0720. This star is found to be seriously contaminated by cirrus emission, and extended structures have been detected around it in all four *IRAS* bands (12, 25, 60, 100 μm). Hence, the observed spectral energy distribution of this star no longer represents that of a single shell.

The $\dot{M}$-L_* relation is shown in Figure 4. In this figure, the type E stars seem to distribute in an area different from that

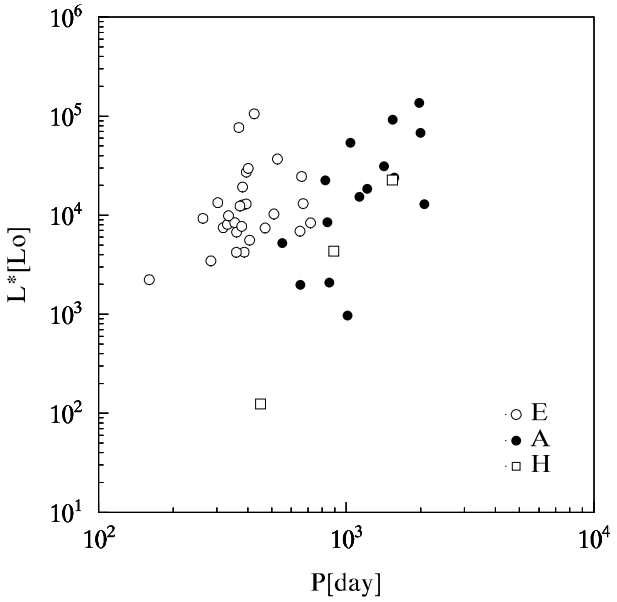


FIG. 2.—Same as Fig. 1, but for the whole sample

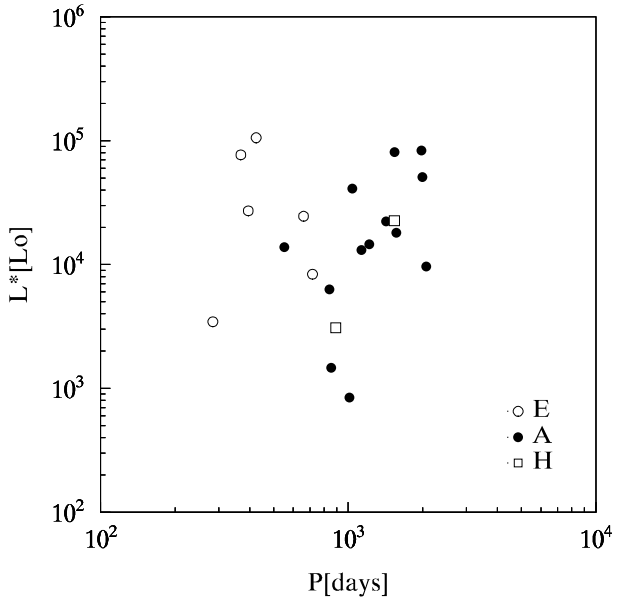


FIG. 1.—The L_*-P relation for the phase-lag sample. The luminosity shown is obtained by modeling.

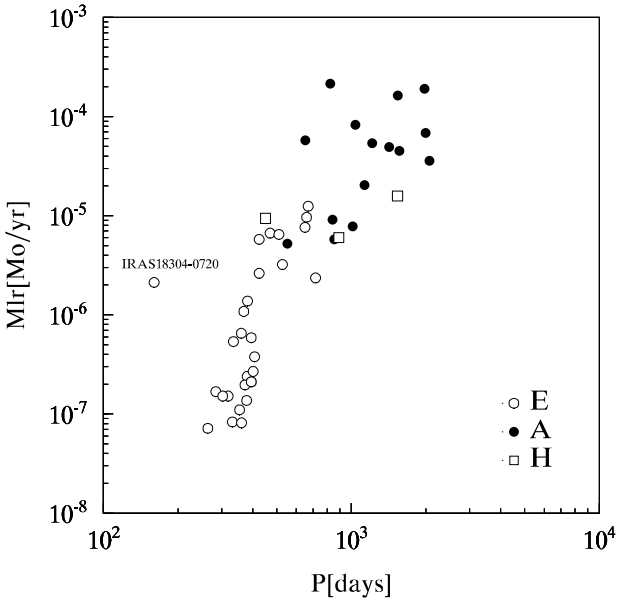


FIG. 3.—The $\dot{M}$-P relation for the OH/IR stars with known outflow velocity of the whole sample. The mass-loss rate shown is obtained by modeling.

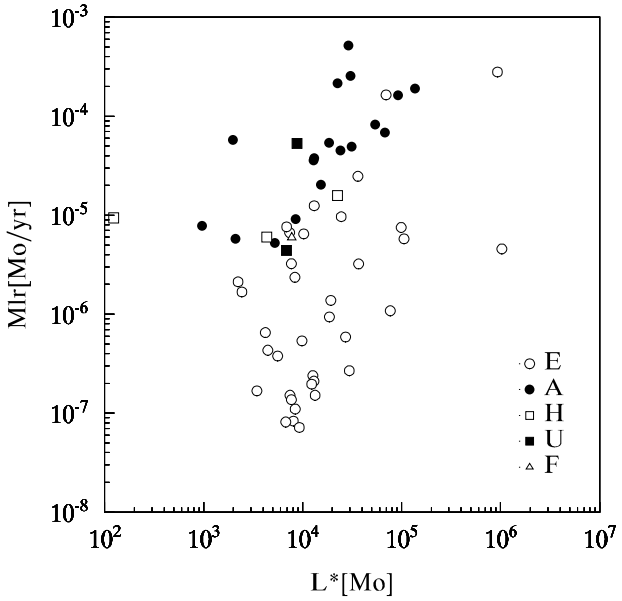


FIG. 4.—Same as Fig. 3, but for the $\dot{M}$-L_* relation. The mass-loss rate and luminosity shown are obtained by modeling.

of the stars of other types. Although the luminosity of type E stars can be very large, the mass-loss rate seems always to be smaller than that of the other types with the same luminosity.

From the discussion above, the L_*-P and $\dot{M}$-L_* relations of type E and A stars seem to follow different tracks, while the $\dot{M}$-P relation of all types in the entire sample follows the same track. What do these facts mean for the evolution of OH/IR stars? According to the general evolutionary picture of asymptotic giant branch (AGB) stars, the luminosity and the mass-loss rate should increase with time, and both should be a function of zero-age main-sequence mass ($M_{\rm ZAMS}$) and chemical abundance. If we assume that all OH/IR stars are evolved from progenitors of similar $M_{\rm ZAMS}$ and chemical abundance, and the type E ones are the precursors of the type A ones as we expected, it is reasonable to expect that both the luminosity and the mass-loss rate of the type E ones should be smaller than that of the type A ones. But in Figure 4, many type E stars can reach high luminosity while their mass-loss rates are always smaller than that of the type A stars with the same luminosity. From Figures 1, 2, 6, and 7, we can also see that some type E stars can evolve into luminous objects even if their period is shorter than type A ones. This hints that some of the two types of OH/IR stars may not evolve from the same population of progenitors (with similar $M_{\rm ZAMS}$ and chemical abundance). If this is the right, we can safely infer from the single $\dot{M}$-P relation obeyed by the whole sample that the differences in $M_{\rm ZAMS}$ and chemical abundance of the progenitors have little effect in the $\dot{M}$-P relation of OH/IR stars.

Chen et al. (2001) have argued that there are probably many type E OH/IR stars that would never evolve into type A ones, because they found that type A OH/IR stars are mainly located on the Galactic plane, while many type E stars are located at high Galactic latitude (see their Fig. 5). Here a similar figure is given in Figure 5*a*, which shows a similar distribution of different types of OH/IR stars. In

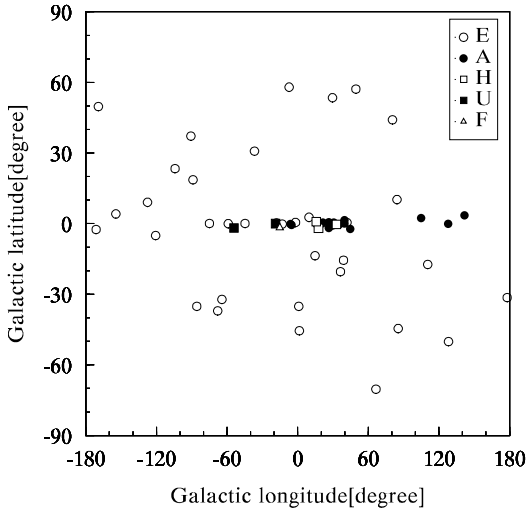


FIG. 5*a*

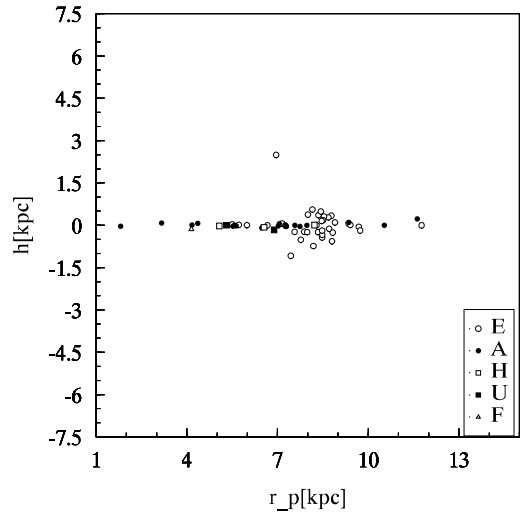


FIG. 5*b*

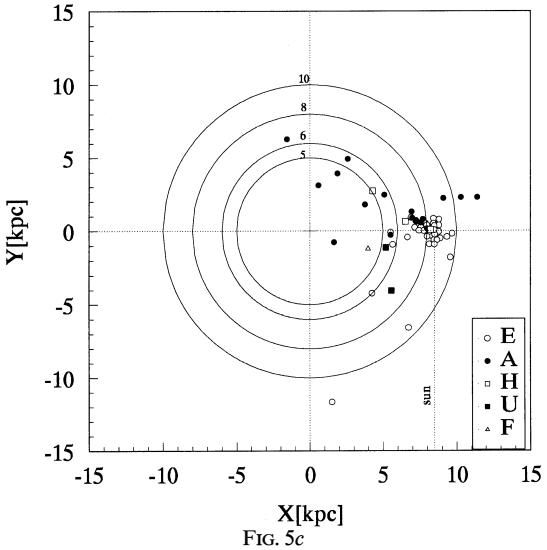


FIG. 5*c*

FIG. 5.—(*a*) Space distribution of the enire sample on the Galactic coordinates. (*b*) Distances of stars to the Galactic plane and the Galactic center; h is the distance to the Galactic plane, and r_p is the distance from the projections of stars on the Galactic plane to the Galactic center. (*c*) Projections of sample stars on the Galactic plane. The Galactic center is marked by a plus sign, and the position of the Sun is marked out by a dotted line. Numbers beside those circles denote the radius of them in kiloparsecs.

addition, more detailed position information of these stars is also shown in Figures 5*b* and 5*c*. The distances from the stars to the Galactic plane and from the projection of these stars on the Galactic plane to the Galactic center are plotted in Figure 5*b*, while the projection of these stars on the Galactic plane is shown in Figure 5*c*. It is indicated from Figure 5 that the majority of type E sample stars are nearby sources while the other types distribute over a larger area. There are three Galactic arms near the Sun: the one at several dozen parsecs outside the solar circle is the Orion arm, the one at about 2 kpc outside the solar circle is the Perseus arm, and another at about 2 kpc inside the solar circle is the Sagittarius arm. From Figure 5*c*, it is reasonable to suppose that many type A sample stars are located in the three Galactic arms. Those stars whose distance to the Galactic center is smaller than about 5 kpc must be located inside the dense galactic H I cloud disk. And those type E stars are located either in the interarm area on the Galactic plane like the Sun or outside of the Galactic plane. From the space distribution of the sample stars, it is not difficult to conclude that, in the whole sample, the type E and other type stars are probably formed in different interstellar environment, hence their chemical composition and evolution process can be different. This probably is the original cause of the discrepancy between the L_*-P and $\dot{M}$-L_* relations of the type E and A stars. It should be noted that the distance of many stars are not very accurate, so Figures 5*b* and 5*c* are valuable only for casual reference.

The conclusions described above are mainly based on the quantities derived by modeling. But there exist many uncertainties in the modeling method. The observed data are not very certain, because of the variation of light, interstellar extinction, and emission, and the distances to many OH/IR stars are not very accurate. There are also many uncertainties in the existing radiative transfer modeling, including the uncertain dust optical properties, the unknown dust grain physical status and density distribution, and others factors. The spectrum of the center star should be calculated in more detail by stellar photosphere models instead of using a blackbody spectrum. And many other physical processes, including the dust formation process and the dust-gas interaction process, need to be included in the model.

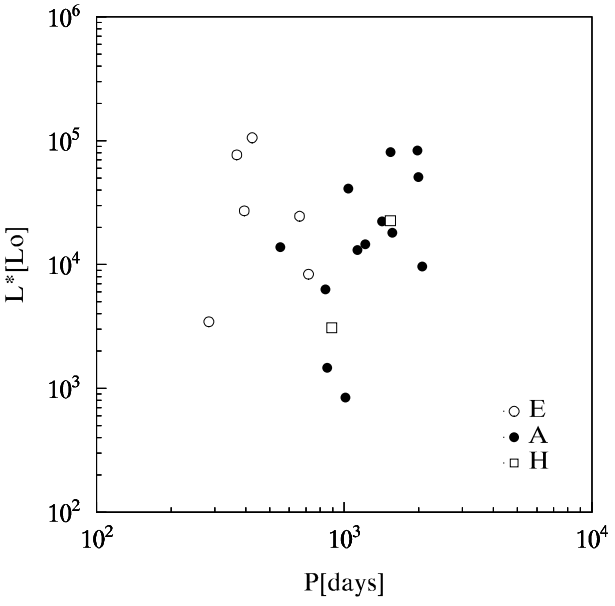


FIG. 6.—The L_*-P relation for the phase-lag sample. The luminosity shown is obtained by directly integrating the observed SEDs.

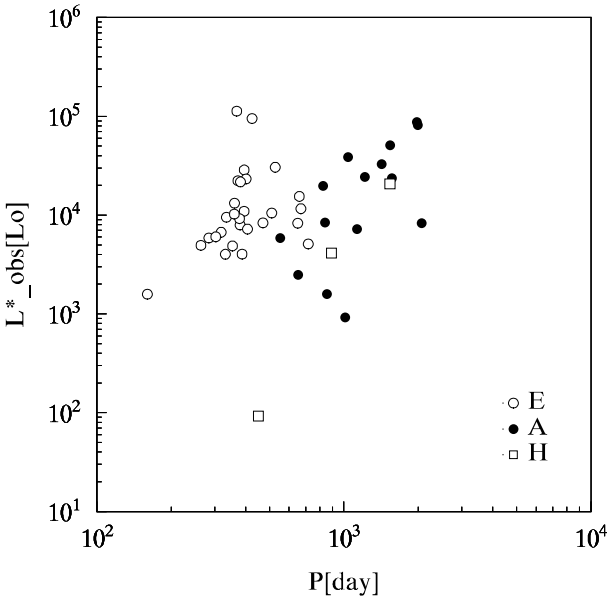


FIG. 7.—Same as Fig. 6, but for the whole sample

Because of these drawbacks of the modeling method, it is reasonable to question the reliability of the derived data such as luminosity and mass-loss rate. In order to clarify the doubts about the derived data, we also calculated the luminosity by directly integrating the observed SEDs. When the spectrum is integrated, it is represented by a blackbody spectrum of temperature 200 K (peak at about 25 μm) in the wavelength range shorter than the first NIR observed data point and longer than 100 μm. The resulting L_*-P relations are shown in Figure 6 for the phase-lag sample and in Figure 7 for the whole sample. In these two figures, the conclusion is basically the same. This ensures in some degree the reliability of the data derived by modeling and the conclusions derived from them.

Another problem should also be noted: Some of the sample stars, even some type E ones, have very high luminosities (about 10^5 $L_\odot$); this is unusual for OH/IR stars. In order to verify whether any calculation errors have occurred, the luminosity data of some sample stars were compared with that from van Langevelde et al. (1990), who had estimated luminosity for some OH/IR stars with phase-lag distances in another way. The luminosity data derived in this paper are found to be comparable to theirs. And there are also some stars in their paper reach a high luminosity near to 10^5 $L_\odot$. It is reasonable to suspect that these luminous stars may actually be supergiants, but further inspection is needed for this subject.

We thank Professor R. Szczerba, who kindly provided us the radiative transfer code. We also have used in our work the on-line SIMBAD database and the on-line *IRAS* Data Analysis Facility at the University of Calgary. This work is supported by grants from the National Natural Science Foundation of China and the Chinese Academy of Sciences.

REFERENCES

Baud, B., & Habing, H. J. 1983, A&A, 127, 73
Baud, B., Sargent, A. I., Werner, M. W., & Bentley, A. F. 1985, ApJ, 292, 628
Blommaert, J. A. D. L., van der Veen, W. E. C. J., van Langevelde, H. J., Habing, H. J., & Sjouwerman, L. O. 1998, A&A, 329, 991
Bowers, P. F., Johnston, K. J., & Spencer, J. H. 1983, ApJ, 274, 733
Cardelli, J. A., Clayton, G. C., & Mathis, J. S. 1989, ApJ, 345, 245
Chen, P.-S., Szczerba, R., Kwok, S., & Volk, K. 2001, A&A, 368, 1006
Draine, B. T. 1985, ApJS, 57, 587
Draine, B. T., & Lee, H. M. 1984, ApJ, 285, 89
Evans, N. J., II, & Beckwith, S. 1977, ApJ, 217, 729
Fix, J. D., & Mutel, R. L. 1984, AJ, 89, 406
Fouqué, P., Le Bertre, T., Epchtein, N., Guglielmo, F., & Kerschbaum, F. 1992, A&AS, 93, 151
García-Lario, P., Manchado, A., Pych, W., & Pottasch, S. R. 1997, A&AS, 126, 479
Gehrz, R. D., Hackwell, Grasdalen, G. L., J. A., Kleinmann, S. G., & Mason, S. 1985, ApJ, 290, 296
Herman, J., Burger, J. H., & Penninx, W. H. 1986, A&A, 167, 247
Jones, T. J., Hyland, A. R., & Gatley, I. 1983, ApJ, 273, 660
Kwok, S., Hrivnak, B. J., & Boreiko, R. T. 1987, ApJ, 321, 975
Le Bertre, T. 1993, A&AS, 97, 729
Lepine, J. R. D., Ortiz, R., & Epchtein, N. 1995, A&A, 299, 453
Le Sidaner, P., & Le Bertre, T. 1996, A&A, 314, 896
Mathis, J. S., Rumpl, W., & Nordsieck, K. H. 1977, ApJ, 217, 425
Nguyen-Q-Rieu, Laury-Micoulaut, C., Winnberg, A., & Schultz, G. V. 1979, A&A, 75, 351
Nyman, L.-Å., Hall, P. J., & Le Bertre, T. 1993, A&A, 280, 551
Ortiz, R., & Maciel, W. J. 1996, A&A, 313, 180
Schultz, G. V., Kreysa, E., & Sherwood, W. A. 1976, A&A, 50, 171
Sun, J., & Zhang, H.-Y. 1998, Acta Astrophys. Sinica, 18, 313 (English transl. Chinese Astron. Astrophys., 22, 442)
Szczerba, R., Omont, A., Volk, K., Cox, P., & Kwok, S. 1997, A&A, 317, 859
van Herk, G. 1965, Bull. Astron. Inst. Netherlands, 18, 71
van Langevelde, H. J., van der Heiden, R., & van Schooneveld, C. 1990, A&A, 239, 193
Whitelock, P., Feast, M., & Catchpole, R. 1991, MNRAS, 248, 276
Whitelock, P., Menzies, J., Feast, M., Marang, F., Carter, B., Roberts, G., Catchpole, R., & Chapman, J. 1994, MNRAS, 267, 711
Xiong, G.-Z., Chen, P.-S., & Gao, H. 1994, A&AS, 108, 661